

Commensurability effects in lateral surface-doped superlattices

R. A. Deutschmann,^{a)} C. Stocken, W. Wegscheider,^{b)} M. Bichler, and G. Abstreiter
Walter Schottky Institut, TU München, Am Coulombwall, 85748 Garching, Germany

(Received 6 December 2000; accepted for publication 15 February 2001)

We fabricate density-modulated two-dimensional electron systems by shallow compensation doping the donor layer of a modulation-doped heterostructure. Zinc acceptor atoms are diffused from the sample surface which is heated by a focused laser beam. Low-temperature magnetotransport experiments provide evidence that high-quality lateral surface superlattices can be fabricated. In weak periodic one-dimensional potentials, commensurability oscillations are recovered, whereas in strong periodic two-dimensional potentials the semiclassically expected antidot resistance resonances are found to dominate the low-field transport. Additionally, the homogeneity of the laser-induced doping is confirmed by magnetic focusing experiments. © 2001 American Institute of Physics. [DOI: 10.1063/1.1362283]

Semiconductor superlattices have long been a fascinating system to study the influence of an artificial potential modulation on an electronic system.¹ In lateral surface superlattices (LSSLs), a two-dimensional electron system (2DES), for example, a modulation-doped GaAs/Al_xGa_{1-x}As heterostructure, is patterned in order to achieve an electron density modulation. Known methods employ holographic illumination,² lithographically defined metallic top gates,³ shallow etching,⁴ laser interference melting,⁵ atomic force microscope surface oxidation,⁶ and growth on vicinal and patterned surfaces.^{7,8} Striking commensurability effects between the electron cyclotron radius and the period length of the superlattice were uncovered in these LSSLs with one-dimensional (1D)^{2,3,8} and two-dimensional (2D)⁹ modulation in low-field magnetotransport experiments.

In this letter, we fabricate lateral surface-doped superlattices (LSDSLs) by local and shallow compensation doping the silicon donor layer of a GaAs/Al_xGa_{1-x}As heterostructure. The versatility of this method is demonstrated by three different examples of commensurability effects in two-dimensional electron systems. First, in weak 1D LSDSLs the known Weiss oscillations^{2,3} at low magnetic fields are recovered, a fact which provides evidence of the high homogeneity of the laser-doped lines. At increased compensation doping concentrations in 2D LSDSLs, typical antidot resonances⁹ are found, demonstrating that high electron mobilities are preserved. In magnetic focusing experiments elongated lines in this high compensation doping regime are shown to be specular reflecting, which further confirms their quality.

Our samples were molecular-beam-epitaxy-grown GaAs/Al_{0.3}Ga_{0.7}As modulation-doped heterostructures with the 2DES 60 nm below the surface. The electron density could be varied between $n_s = 3.5 \times 10^{11} \text{ cm}^{-2}$ and $n_s = 6.1 \times 10^{11} \text{ cm}^{-2}$ by successive illumination with a red light-emitting diode, electron mobility at the latter density was $1.6 \times 10^6 \text{ cm}^2/\text{V s}$. All experiments were performed at liquid-

helium temperatures using the four-point lock-in measurement technique with a measurement current of $I = 1 \mu\text{A}$. Compensation doping was achieved by heating the Zn:SiO₂ capped sample surface with the highly focused beam of an Ar⁺ laser (wavelength 458 nm, laser power 1–100 mW). A nonlinear thermally activated diffusion process results in local compensation doping of the initial *n*-type silicon doping layer by *p*-type zinc atoms, and, most importantly, in a significant narrowing of the lateral doping profile as compared to the initial laser spot profile.¹⁰ Calculated diffusion depths of the zinc atoms are between a few and 20 nm, depending on the used laser power.¹⁰ It is, therefore, expected that ionized impurity scattering is hardly increased after laser patterning. Using this method, Baumgartner and co-workers have previously fabricated in-plane-gated devices such as quantum-point contacts, single-electron transistors, and Aharonov–Bohm rings.^{11,12}

In order to determine possible period lengths and modulation amplitudes in our LSDSLs, we have performed self-consistent Poisson/Schrödinger calculations of the 2DES at the presence of compensation doping in the initial *n*-type doping layer. At a measured laser spot full width at half maximum (FWHM) of 315 nm, the calculated resulting doping profile is Gaussian shaped with a FWHM of 105 nm,¹⁰ and the maximum *p*-doping concentration in the center p_0 depends on the laser power. We find that for $n_s = 4.3 \times 10^{11} \text{ cm}^{-2}$ and $p_0 = 8 \times 10^{10} \text{ cm}^{-2}$ the potential modulation is 7% of the Fermi energy with a FWHM of 112 nm, while for $p_0 = 1.2 \times 10^{12} \text{ cm}^{-2}$ at the same electron density the 2DES is depleted, but the FWHM is hardly increased to 122 nm, see Fig. 1. These results indicate that LSDSL with periods even below the laser spot size should be achievable.

In a first set of experiments we have successfully fabricated LSDSLs with 1D modulation and periods between $d = 500 \text{ nm}$ and $d = 200 \text{ nm}$ by laser writing an array of 10- μm -long lines across a small Hall bar. The same laser power as used for the calculation shown in Fig. 1(a) was chosen. Measurement results of a sample with $d = 300 \text{ nm}$ are shown in Fig. 2 for two different temperatures $T = 4.2 \text{ K}$ and $T = 1.5 \text{ K}$. At magnetic fields below $B = 1 \text{ T}$ Weiss oscillations^{2,3} with their typical weak temperature depen-

^{a)}Electronic mail: deutschmann@wsi.tum.de

^{b)}Present address: Universität Regensburg, Universitätsstrasse 31, 93040 Regensburg, Germany.

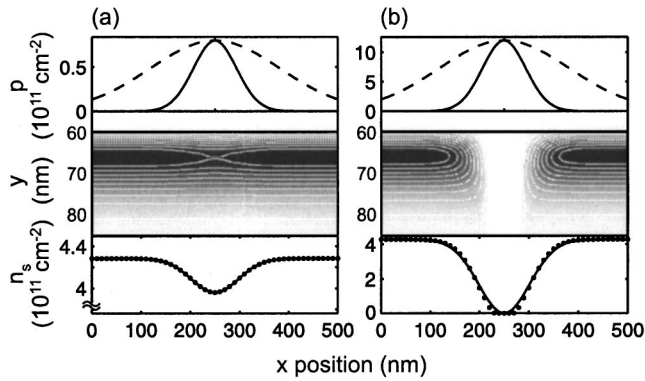


FIG. 1. Top: scaled laser-beam profile (dashed) and doping concentration (solid); middle: calculated electron concentration gray scale encoded (black: $3.57 \times 10^{17} \text{ cm}^{-3}$, white: $0 \times 10^{17} \text{ cm}^{-3}$); bottom: integrated 2D charge density n_s (circles) and Gaussian fit (solid line). (a) Small laser power, $p_0 = 8 \times 10^{10} \text{ cm}^{-2}$; (b) large laser power, $p_0 = 1.2 \times 10^{12} \text{ cm}^{-2}$. Depending on the laser power, small and large potential modulations can be fabricated, while the width of the electron depletion zone remains almost constant, and much below the laser spot size.

dence are clearly resolved as $1/B$ periodic oscillations in the longitudinal magnetoresistance. They are explained in a semiclassical picture as a resonance in the $E \times B$ drift of the cyclotron orbit center,¹³ or quantum mechanically by an oscillating bandwidth of the modulation-broadened Landau levels.^{2,3} Given the period and electron density, which we determine from the high-field Shubnikov–de Haas oscillations, the expected positions $B^{(i)}$ of the resistance minima $i = 1, 2, \dots$,

$$B^{(i)} = \frac{2\hbar \sqrt{2\pi n_s}}{ed(i-1/4)},$$

marked by arrows in Fig. 2, coincide well with the experimental data. Potential modulation amplitudes evaluated both using the semiclassical model¹³ and the magnetic breakdown picture¹⁴ mutually agree well with a magnitude of 7% of the Fermi energy.

In a second set of experiments two-dimensional LSDSLs were fabricated by laser writing a $10 \mu\text{m} \times 10 \mu\text{m}$ square array of dots in a small Hall bar at a laser power corresponding to Fig. 1(b). Clear resistance maxima are found at magnetic-

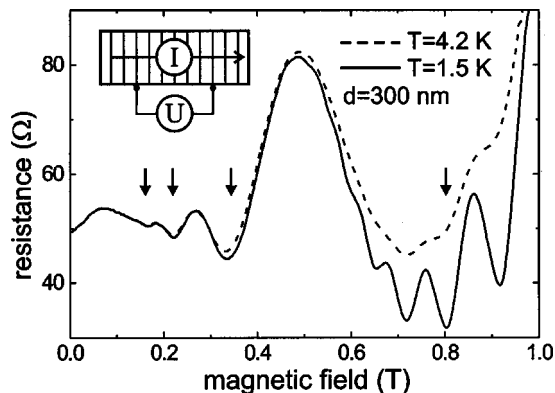


FIG. 2. Commensurability oscillations in the 1D LSDSL with period $d = 300 \text{ nm}$ at $n_s = 3.1 \times 10^{11} \text{ cm}^{-2}$ for two different temperatures. The inset schematically shows the measurement scheme for the longitudinal magnetoresistance. Arrows indicate the theoretically expected location of resistance minima. Shubnikov–de Haas oscillations appear as $1/B$ periodic features above $B = 0.6 \text{ T}$.

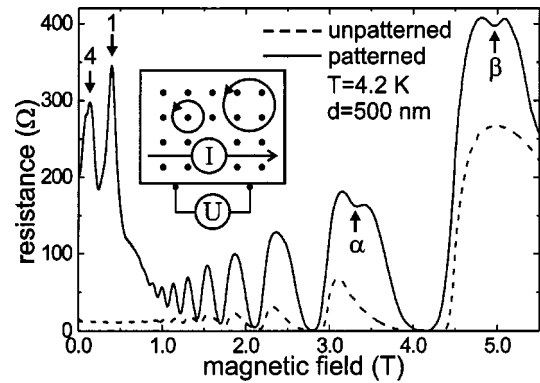


FIG. 3. Commensurability oscillations in the rectangular 2D LSDSL at $n_s = 3.9 \times 10^{11} \text{ cm}^{-2}$. Resistance resonances originate from electron localization around one and four antidots, as indicated by the arrows and shown schematically in the inset. Features marked by α and β cannot easily be explained by semiclassical orbits.

field strengths corresponding to electron cyclotron orbits around one and four antidots with $d = 500 \text{ nm}$, as indicated by arrows in Fig. 3, in agreement with a simple electron pinball model.⁹ The small dips α and β in the Shubnikov–de Haas maxima at smaller filling factors were reproducible in different cooldowns and different samples. Their position forbids the trivial explanation by spin splitting, for example, the dip denoted by β lies between filling factors 3 and 4. They may be signatures of the band structure induced by the lateral antidot lattice.

In addition to the first set of experiments, where the presence of Weiss oscillations indicated highly homogeneous laser written lines in the weak potential modulation regime, a third set of experiments was set up to determine the quality of laser-written lines in the strong potential modulation regime. For that reason, we have performed magnetic focusing experiments in a $10 \mu\text{m} \times 10 \mu\text{m}$ square of electrically isolating laser-written lines with small openings at the corners, as shown in Fig. 4. Clear magnetoresistance oscillations periodic in B are caused by electrons that are specularly reflected at the boundary up to five times.¹⁵ We have experimentally confirmed the expected length dependence of the resonances in a structure with a sidewall

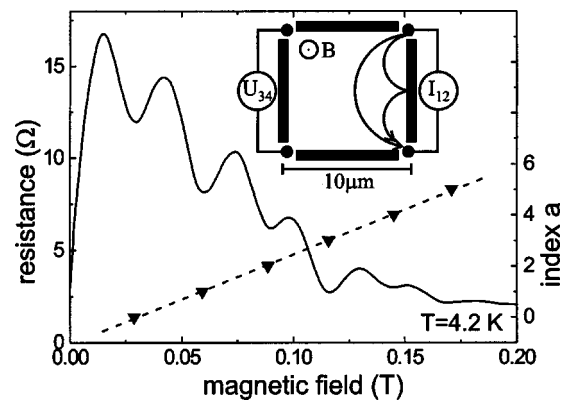


FIG. 4. Commensurability oscillations in the laser-doped magnetic focusing structure. Observed resistance oscillations demonstrate the commensurability between the electron cyclotron radius and the $10 \mu\text{m}$ sidewall where the electron bounces an integer number of times a , as schematically shown in the inset for $a = 0$ and $a = 1$. The periodicity in magnetic field of the resonances is well confirmed by a linear fit through the position of the resistance minima (dashed line).

length of 5 μm , where resonances appeared at double the magnetic-field strengths. The result of this experiment further demonstrates the smoothness of the laser-generated potential modulation.

In summary, we have fabricated lateral surface doped superlattices by selectively *p*-type doping an initially *n*-type GaAs/Al_{0.3}Ga_{0.7}As heterostructure with down to sublaser-wavelength periods. Lateral regularity and homogeneity of the laser-written structures were confirmed by magnetotransport measurements on 1D and 2D LSDSLs. In the former case, Weiss oscillations were observed, whereas in the latter case typical antidot resonances appeared. The high quality of the laser-written lines was further demonstrated by magnetic focusing experiments, showing specular reflection of electrons of up to five times. In contrast to other patterning methods, with our method of compensation doping almost arbitrary lateral potential landscapes may be fabricated. This is simply achieved by adjusting the laser power during the patterning process. LSDSLs with complex unit cells not only in lateral shape but also in electron density should be feasible. We have demonstrated two particular examples of weak and strong modulation strengths. With our method, little or no crystal damage occurs during patterning, and mechanical strain, which often interferes with the electrostatic modulation using other methods, is avoided. Our LSDSLs may additionally be gated for further flexibility.

The authors gratefully acknowledge valuable help by M. Huber and the support by the Deutsche Forschungsgemeinschaft via SFB 348.

- ¹L. Esaki and R. Tsu, IBM J. Res. Dev. **14**, 61 (1970).
- ²R. R. Gerhardts, D. Weiss, and K. v. Klitzing, Phys. Rev. Lett. **62**, 1173 (1989).
- ³R. W. Winkler, J. P. Kotthaus, and K. Ploog, Phys. Rev. Lett. **62**, 1177 (1989).
- ⁴A. R. Long, E. Skuras, S. Vallis, R. Cuscó, I. A. Larkin, J. H. Davies, and M. C. Holland, Phys. Rev. B **60**, 1964 (1999).
- ⁵C. E. Nebel, J. Rogg, M. K. Kelly, B. Dahlheimer, M. Rother, M. Bichler, W. Wegscheider, and M. Stutzmann, J. Appl. Phys. **82**, 1497 (1997).
- ⁶R. Held, T. Vancura, T. Heinzel, K. Ensslin, M. Holland, and W. Wegscheider, Appl. Phys. Lett. **73**, 262 (1998).
- ⁷F. Petit, L. Sfaxi, F. Lelarge, A. Cavanna, M. Hayne, and B. Etienne, Europhys. Lett. **38**, 225 (1997).
- ⁸R. A. Deutschmann, A. Lorke, W. Wegscheider, M. Bichler, and G. Abstreiter, Physica E (Amsterdam) **6**, 561 (2000); R. A. Deutschmann, W. Wegscheider, M. Rother, M. Bichler, G. Abstreiter, C. Albrecht, and J. H. Smet, Phys. Rev. Lett. **86**, 1857 (2001).
- ⁹D. Weiss, M. L. Roukes, A. Menschig, P. Grambow, K. v. Klitzing, and G. Weimann, Phys. Rev. Lett. **66**, 2790 (1991).
- ¹⁰P. Baumgartner, K. Brunner, G. Abstreiter, G. Böhm, G. Tränkle, and G. Weimann, Appl. Phys. Lett. **64**, 592 (1994).
- ¹¹P. Baumgartner, W. Wegscheider, M. Bichler, G. Schedelbeck, R. Neumann, and G. Abstreiter, Appl. Phys. Lett. **70**, 2135 (1997).
- ¹²P. Baumgartner, W. Wegscheider, M. Bichler, G. Groos, and G. Abstreiter, Physica E (Amsterdam) **2**, 441 (1998).
- ¹³C. W. J. Beenakker, Phys. Rev. Lett. **62**, 2020 (1989).
- ¹⁴P. H. Beton, M. W. Dellow, P. C. Main, E. S. Alves, L. Eaves, S. P. Beaumont, and C. D. W. Wilkinson, Phys. Rev. B **43**, 9980 (1991).
- ¹⁵H. van Houten, C. W. J. Beenakker, J. G. Williamson, M. E. I. Broekaart, P. H. M. v. Loosdrecht, B. J. v. Wees, J. E. Mooij, C. T. Foxon, and J. J. Harris, Phys. Rev. B **39**, 8556 (1989).